

EXPERIMENTAL DETERMINATION AND MICROMECHANICAL
MODELLING OF DAMAGE IN NODULAR CAST IRON

W. Baer², D. Steglich¹, W. Brocks¹, G. Pusch²

Two ferritic nodular cast iron materials of the type GGG-40 with different graphite morphology were investigated. Tensile tests with smooth and notched specimens were carried out to experimentally examine the load-deformation behaviour. The fracture behaviour was determined by testing SE(B)-specimens. The numerical simulations were realized within the FE-program ABAQUS by a user supplied material model of porous metal plasticity proposed by Gurson, Tvergaard and Needleman. Fracture resistance curves could be simulated by these means. The amount of damage in tensile specimens was experimentally quantified and compared with the predictions of the FE-calculations.

INTRODUCTION

The increasing application of nodular cast iron in structures and components requires a detailed characterization of this material to predict its toughness and damage behaviour at static loading in dependence of the graphite morphology. The application of micromechanical damage models extended the methods of safety assessment avoiding the problems of geometry dependent parameters as in conventional fracture mechanics.

Nodular cast iron has nearly ideal microstructure for microscopical investigations. The diameter of the spherical or elliptical graphite inclusions is about 10 μm to 100 μm . Thus, material damage could be determined by optical microscopy and the results could be compared with numerical predictions based on micromechanical damage models.

- ¹⁾ GKSS Research Centre, Inst. for Materials Research, Max-Planck-Str.,
D-21502 Geesthacht
- ²⁾ TU Mining Academy Freiberg, Inst. for Materials Technology,
Gustav-Zeuner-Str. 5, D-09599 Freiberg

TESTING MATERIALS

Two different materials with different graphite morphology were investigated which had been taken from transport containers for waste nuclear fuel rods. First, a material with nearly spherical inclusions (GGG-40/1AZ) was tested to investigate the effect of particle size on the evolution of damage. A second material with more ellipsoidal inclusions (GGG-40/3AZ) was investigated to determine the effects of the particle shape. Table 1 shows the mechanical and microstructural parameters of the two materials.

A separate description of the mechanical behaviour of the matrix material and the graphite inclusions is necessary for the micromechanical modelling. The manufacturing of a ferritic bulk material which has the same mechanical properties as the matrix material in cast iron required special efforts. The procedure started from the ferritic mild steel Mk3Al in hot rolled state. The content of silicon was adjusted to that of cast iron by alloying ferro-silicon FeSi75 by means of fusion metallurgy. Special care has to be taken to prevent the silicon from burning off. Iron silicon alloys of this composition do not show phase transformation up to the melting point. Thus the coarse grained microstructure could only be changed by hot rolling down to a grain size which is similar to that of the considered cast iron.

TABLE 1 - Mechanical and microstructural properties

Material	$R_{p0.2}$ MPa	R_m MPa	E GPa	f_0, V_v [%]	λ [mm]	S_F
GGG-40/1AZ	277	416	158	11.4	51	0.85
GGG-40/3AZ	278	387	166	12	96	0.70
Mk3Al	243	340	215	-	-	-
FeSi-Matrix- alloy	366 (R_{eL})	530	195	-	-	-

V_v = volume fraction of the graphite

λ = nearest neighbour distance

S_F = shape factor ($S_F = 4\pi A/U^2$)

A = cross section of the particle

U = circumference of the particle

Graphite cannot bear tensile stresses. Therefore decohesion between matrix material and spherulitic graphite can be observed at low stresses, i.e. 30-50% of the macroscopic yield stress (Baer and Pusch (1)). Debonding can take place at the boundary either between graphite sphere and matrix or between primary and secondary graphite close to the surface of the graphite sphere.

EXPERIMENTAL DETERMINATION OF DAMAGE

The metallographic investigation of damage in the material are based on the analysis of pores, where a pore has to be understood as the entirety of graphite inclusion and nucleated void. Starting from the initial value of damage, f_0 , which corresponds to the void volume fraction of graphite, damage is increasing with increasing load.

The void volume fraction was measured on polished specimens by using the image analysis system IMAGE C with observation windows of $500 * 500 \mu\text{m}^2$. A mean value out of 10 to 15 adjacent observation windows in the center of the round specimen close to the longitudinal axis was calculated. Plotting these values along the longitudinal axis yields the distribution of damage with the reference value f_0 at the specimen head.

Some specimens were stressed up to fracture and some tests were stopped at lower strain states to obtain informations about the evolution and distribution of damage in the tensile bars by metallographic analyses. Any determination of the void volume fraction close to the notch of notched bars appeared not to make sense because of the high gradients of damage due to the high triaxiality in this region.

MODELLING OF THE MATERIAL BEHAVIOUR

The damage model of GURSON (2), TVERGAARD and NEEDLEMAN (3) (GTN model) describes the micromechanical processes of void nucleation, growth and coalescence which dominate ductile crack growth. Based on the yield condition of v. MISES the model includes a second internal variable, f , which can be identified as the void volume fraction. A macroscopic crack occurs when a certain void volume fraction is exceeded at one point. This model has been implemented as user supplied routine (Hao and Brocks (4)) in the FE program ABAQUS.

As decohesion between the ferritic matrix and the graphite occurs at low strains, the nucleation of voids must not be modelled in the present application, The

volume fraction of the graphite was hence taken as the initial value of damage, f_0 . The effect of different shapes of the inclusions on void growth and coalescence was studied by cell model calculations on unit cells with nearly spherical (GGG-40/1AZ) and ellipsoidal (GGG-40/3AZ) shaped voids. v. Mises yield condition and isotropic hardening of the matrix material are assumed for these calculations. The corresponding stress-strain curve was obtained from tensile tests with the purely ferritic material. The mesoscopic stress-strain relation of the unit cell and the critical void volume fraction, f_c , which describes the plastic collapse of the cell are obtained as results (Koplik and Needleman (5)).

RESULTS

The variation of damage along the axis of a round tensile bar which was determined as described above is compared in Figure 1 with the results of the numerical simulation. A high gradient of damage with a maximum value of 18 % is observed in the region of localised deformation of the broken cracked specimen which could be simulated very well. The FE-simulation also shows a gradient of damage in radial direction, so that damage decreases from the centre to the surface of the specimen.

Figure 2 shows the macroscopic quantities force and reduction of diameter of a notched round specimen ($D=14$ mm, $d=8$ mm, $\rho=4$ mm) obtained with the GTN-model in comparison with experimental data. Fracture in the experiment occurred at nearly the same deformation for both materials, just the values of the force are slightly different. Because of the high triaxiality the differences in initial void volume fraction (1AZ: 11.4%, 3AZ: 12%) have little effect on the force at fracture in the numerical model. The specimen made of GGG-40/3AZ fails at a lower strain in the simulation due to its higher rate of graphite.

Finally, Figure 3 shows experimental and numerical J_R curves of SE(B) specimens which coincide quite well. Fracture resistance increases with increasing spacing of graphite inclusions. While the size of the finite elements at the crack tip for simulation of the material GGG-40/1AZ was $0.3 * 0.4$ mm², it was set to $0.6 * 0.8$ mm² for simulating the specimen made of GGG-40/3AZ. Thus, the element length correlates with the microstructure and is six times the nearest neighbour distance of the inclusions in both cases.

REFERENCES

- (1) Baer, W. and Pusch, G., "Investigation of Fracture Mechanical Performance of Nodular Cast Iron and Welded Joints with Parent-Material-like Weld Metal", Fracture Mechanics: 26th Volume, ASTM STP 1256, W.G. Reuter, J.H. Underwood and James C. Newman, Jr., (eds.), American Society for Testing and Materials, Philadelphia, 1995.
- (2) Gurson, A. L., J. Engng. Mater. Tech., Vol. 99, 1977, pp. 2-15.
- (3) Needleman, A. and Tvergaard, V., J. Mech. Phys. Solids, Vol. 32, 1984, pp. 461-490.
- (4) Hao, S. and Brocks, W., "The Gurson-Tvergaard-Needleman Model for rate- and temperature-dependent material with isotropic und kinematic hardening", Technical Note GKSS/WMG/95/1, GKSS Research Centre , 1995.
- (5) Koplik, J. and Needleman, A., Int. J. Solids Structures, Vol. 24, 1988, pp. 835-853.

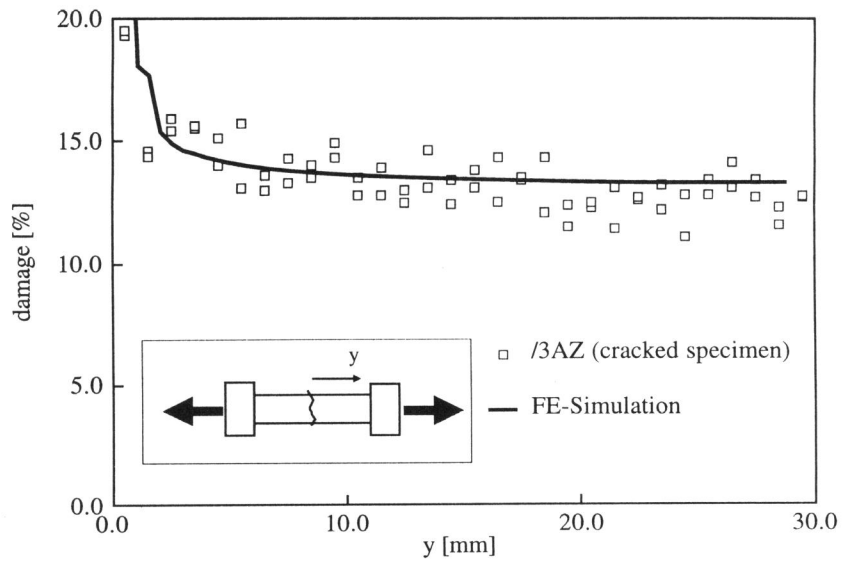


Figure 1. void volume fraction, experiment and FE-simulation

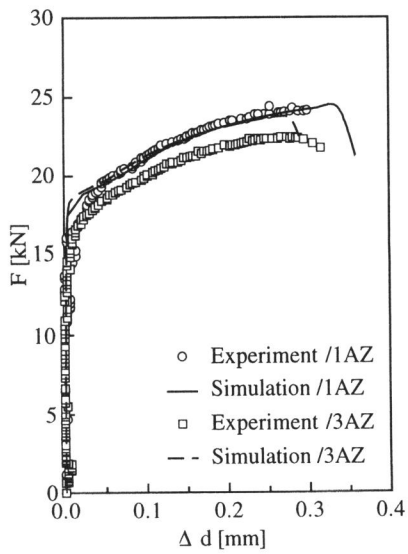


Figure 2. tensile test of round notched specimen, force vs reduction of diameter

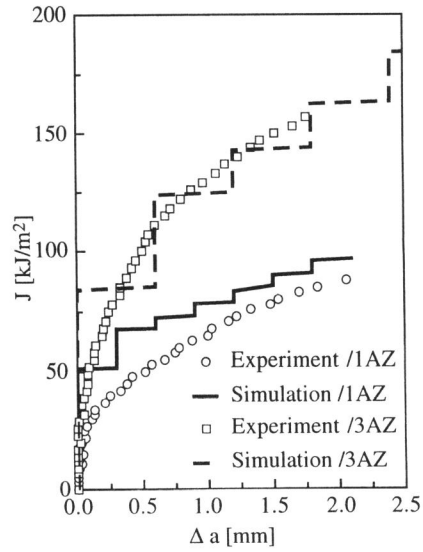


Figure 3. SE(B)-specimen, J_R -curves